

Modeling the Photophoretic Force and Brownian Motion of a Single Sphere

Jeremy L. Smallwood and Lorin S. Matthews

Abstract— The details of planet formation are still largely unknown. A number of forces play a role in the coagulation process, where solid material in a protoplanetary disk grows from micrometer sized dust grains to kilometer sized objects. One force which could be important is the photophoretic force. Dust grains illuminated by the central star will be unevenly heated. As gas molecules come into contact with the warmer side of the grain, they are re-emitted with a higher velocity. This difference in momentum transfer due to the temperature gradient induces a net force which is directed away from the illumination, in this case, away from the star, with the magnitude of the force increasing with the temperature gradient across the grain. This may explain a feature of our own solar system, where the density of the planets decreases with increasing distance from the sun (Mercury is metallic and Earth is rocky). Metallic grains are thermally conducting and thus develop a smaller temperature gradient versus non-metals, thus more metallic grains may stay near the star while non-metallic grains are pushed outward. This study examines the photophoretic force on aggregates in a laboratory environment. Dust aggregates consisting of micron-sized spheres are illuminated with a laser. A high-speed camera is used to record the motion of the dust aggregates and to determine the magnitude of the force. Numerical simulations are also used to model the resultant motion and the photophoretic force. The results are then compared to experimental data.

Index Terms— aggregates, dusty plasma, photophoresis, protoplanetary disk

I. INTRODUCTION

PLANET formation depends primarily on the combining, or coagulation, of dust grains. Dust grains are found orbiting in a protoplanetary disk around a newborn star. Along with dust grains, protoplanetary disks also comprise of gas molecules that continually come into contact with the dust grains. It is important to study how these micron-sized grains can eventually form a planet because it can reveal more information about the formation of our own solar system. Many forces play a role in the dynamics of dust grains which leads to the structure observed in our solar system and others. Examining the movement of these particles will further the understanding of how more dense planets originate closer to the host star (our Sun). One such force that could be responsible for this phenomenon is the photophoretic force, which arises from a process known as photophoresis.

It is observed that the density of the planets in our solar system decreases with increasing distance from the Sun. Looking at the terrestrial planets, mercury is the densest planet

followed by Venus, Earth, and then Mars. Investigation is ongoing to determine why this pattern in densities is present in our solar system. A potential candidate for these observations is the photophoretic force. As stated, metallic grains will have a weaker photophoretic force than silicates. Mercury's composition is much more metallic than Earth, which is rocky. According to Wurm et al. (2013), sorting due to photophoretic forces could cause dense planets to form close to their parent star.

At the time of writing, there are 1491 total confirmed exoplanets (exoplanets.org). Many of the earliest exoplanets detected were Jupiter-sized and found close to their host star on very eccentric orbits. These early observations contradict the structure of our own solar system. This raises the questions of are these other solar systems anomalies or were sorting mechanisms different? Since there are large Jupiter-like exoplanets close to their parent stars, it seems that photophoresis was not present when these solar systems were formed. There also have been observations of rocky exoplanets (CoRoT-78 & Kepler 10b) orbiting close to their parent star. These solar systems may show a similar trend to our solar system, but more data on exoplanets is needed.

II. METHODS

Modeling the trajectories of aggregates due to Brownian motion and photophoresis can give valuable information in the sorting of materials in protoplanetary disks. In this study, we modeled the trajectories of aggregates and single spheres due to Brownian motion and the photophoretic force. Every aggregate modeled is comprised of spherical monomers, for easier calculations and the surface of each monomer is divided into smaller patches. The random force generated from Brownian motion and the photophoretic force are calculated using the *OML-LOS Code*, which will be explained in further detail in the next subsection. The *Dynamics Code* is responsible for tracking the aggregate position, velocity, and acceleration at each time step, and eventually providing a trajectory of the aggregate or single sphere.

A. OML-LOS

The calculation of the photophoretic force on an aggregate depends on a temperature gradient across the

surface of the aggregate and the resulting collisions of gas molecules to that surface. The OML-LOS code calculates the temperature gradient on the aggregate, the reason this code depends on the line-of-sight, is because in an aggregate some patches of monomers are blocked with other monomers. There are points assigned to the surface of each monomer of the aggregate. These points are used to calculate the photophoretic force by calculating illumination, temperature gradient, and momentum transfer.

B. Illumination

In order to obtain a temperature gradient across an aggregate, there needs to be a source of illumination to heat up one side of the aggregate. The illumination direction is along a fixed axis, we commonly use the x-axis. The illumination of each patch, p , is calculated by

$$\Phi_p = \hat{n}_p \cdot \hat{x} \Delta\Omega_p \quad (1)$$

where \hat{n} is the unit normal at the surface of the monomer and $\Delta\Omega$ is the solid subtended angle produced by the area of patch. In order to correctly measure the illumination, the light flux must be in an open LOS with respect to the surface points and not blocked by other monomers. The total illumination flux of an i^{th} monomer is calculated by summing all the illumination fluxes of every patch on the monomer, $\Phi_i = \sum \Phi_p$. The illumination of each monomer generated by the light flux is used to measure the temperature gradient across the aggregate. A pictorial representation of the illumination over an aggregate and isolated sphere is given in figure 1 below.

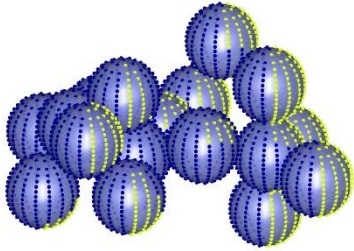


Figure 1. As radiation comes in from right to left, the surface points exposed to the radiation are illuminated greater than the shadow points. (a) Mapping of illuminated of an aggregate.

C. Temperature Gradient

The temperature gradient is not uniformly distributed across the given aggregate based on the difference of illumination flux for each point. The average temperature of the aggregate is based on the average temperature of the gas, T_g . The temperature of each constituent monomer, T_i , is determined by the amount of illuminated patches, thus the illuminated patches will have a higher temperature than the shadow patches. The temperature of each monomer is calculated by:

$$T_i = T_g + \left(\frac{\Phi_i}{\pi} - 0.5 \right) \Delta T \quad (2)$$

where Φ_i is the illumination of the monomer and ΔT is the largest temperature gradient from the largest monomer in the aggregate. In order to calculate the correct half of the temperature gradient of the aggregate, the surface temperature at each illuminated point on the aggregate is calculated,

$$T_p = \bar{T}_i + (\Phi_p / \Phi_{p,max}) x_p \frac{\Delta T}{\Delta x} \quad (3)$$

where Φ_p is the illumination of that point, $\Phi_{p,max}$ the maximum illumination flux to a point on the given monomer, x_p is the x-component of the distance of the point from the center of the monomer, and $\Delta T / \Delta x$ is the temperature gradient in the grain material. To calculate the other half of the temperature gradient, the temperature of each shadow point is calculated,

$$T_p = \bar{T}_i - x_{sh} \frac{\Delta T}{\Delta x} \quad (4)$$

where x_{sh} is the x-component of the distance from the shadow point to the center of that monomer. A representation of the temperature gradient of an aggregate and an isolated sphere is given in figure 2. The temperature gradient results in a transfer of momentum due to collisions of gas molecules.

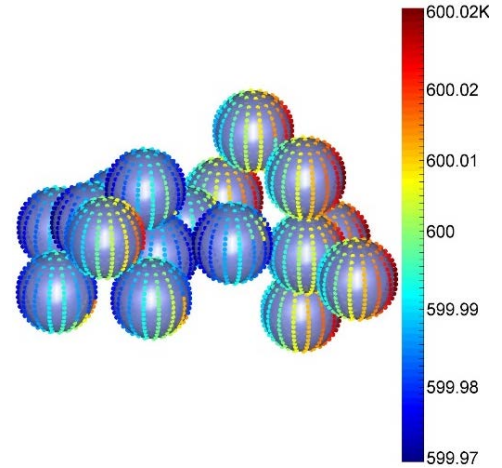


Figure 2. The temperature at each point on the monomers is proportional to the amount of illumination. Above shows the map of the temperature gradient for an aggregate.

D. Momentum Transfer

As gas molecules collide with the points on the aggregate, the gas accommodates to the surface temperature of the point. Gas molecules colliding with the illuminated points will rebound with a higher velocity than the previous incoming velocity. The gas molecules colliding with shadow points will rebound with a lower velocity than illuminated collisions. This difference in incoming and rebounding velocities produce a

transfer of momentum which is used to calculate the photophoretic force and the random force from Brownian motion.

The incoming gas molecules are visualized traveling in a straight path along the open LOS of each point on the aggregate. The number of particles impacting the surface per unit area per unit time is the flux, given by

$$I = n \iiint v \cos \alpha f(v) d^3 \bar{v} \quad (5)$$

where n is the number density of the gas particles, $v \cos \alpha$ is the component of the velocity normal to the surface, and $f(v)$ is the velocity distribution, assumed to be Maxwellian

$$f(v) = \left(\frac{m}{2\pi kT}\right)^{3/2} \exp\left(\frac{-mv^2}{2kT}\right) \quad (6).$$

In the velocity distribution, m is the mass of the gas molecule, k is the Boltzmann constant, and T is the temperature of the gas.

The integrals in the flux can be separated into an integral over the magnitude of the velocity and an integral over the angles,

$$I = n \int_0^\infty v^3 f(v) dv \iint \cos \alpha d\Omega \quad (7)$$

where $\iint \cos \alpha d\Omega$ is known as the LOS factor. The LOS factor depends on the open lines of sight of the aggregate. For an isolated sphere, all the points have an open line of sight except for being blocked by the monomer itself. Since all points have an open line of sight, the limits for the angular integration are $0 \leq \theta \leq \pi/2$ and $0 \leq \phi \leq 2\pi$ and LOS factor = π for all points on the surface. For an aggregate, some of the points have a blocked line of sight. The LOS factor for an aggregate is calculated numerically for each point. The incoming colliding gas molecules have a random incoming direction. If the incoming direction is blocked and is not along the open line of sight, a new incoming direction is calculated until the incoming direction is not blocked.

As the gas accommodates to the surface temperature, the gas molecules are released in a random rebound direction along an open line of sight. If the random rebound direction is blocked, another rebound direction is calculated until it is along an open line of sight. The gas rebounds continue until 99.99% of the gas molecules have rebounded. The transfer of momentum depends on the collisions of incoming and the rebound of gas molecules. If the rebound direction is blocked, the momentum calculated for that situation is not added to the total momentum transfer. Only rebound directions along an open line of sight and initial incoming collisions along a random path with an open line of sight contribute to the momentum transfer. The magnitude of momentum for incoming particles at each point is calculated by,

$$\left(\frac{p_{in}}{\Delta t}\right)_p = I_p m (v_{g,in} D_{i,p} - v_{agg}) A_p \quad (8)$$

where I_p is the flux on patch p , m is the mass of the gas particle, $v_{g,in}$ is the thermal velocity of the incoming gas, calculated below, $D_{i,p}$ is the incoming direction for the gas particle at a patch, v_{agg} is the velocity of the aggregate, and A_p is the area of the patch. The magnitude of momentum for rebounding particles at each point is calculated by,

$$\left(\frac{p_{out}}{\Delta t}\right)_p = I'_p m (v_{g,out} D_{r,p} - v_{agg}) A_p \quad (9)$$

where I'_p corrected gas flux for rebounding particles, $v_{g,out}$ is the thermal velocity of the rebounding gas based on the surface temperature, T_p , and $D_{r,p}$ is the rebound direction for the gas particle at a patch. The thermal velocity of incoming gas and rebound gas particles is calculated below respectively,

$$v_{gas_{in}} = \sqrt{\frac{8kT_g}{\pi m_g}} \quad (10)$$

$$(v_{gas_{out}})_p = \sqrt{\frac{8kT_p}{\pi m_g}} \quad (11)$$

where k is the Boltzmann constant, T_g is the temperature of the gas, m_g is the mass of the gas in kilograms, and T_p is the surface temperature of a patch. From the magnitude of the incoming particles and rebound particles, the magnitude of the force on a chosen patch is calculated by,

$$\mathbf{F}_p = \left(\frac{p_{in}}{\Delta t}\right)_p + \left(\frac{p_{out}}{\Delta t}\right)_p \quad (12).$$

The total force is for the aggregate is calculated by vector summing all the forces on each patch. The photophoretic force is calculated by using the rebound direction based on a temperature gradient and the Brownian motion of the aggregate is calculated by using a rebound direction not dependent on a temperature gradient.

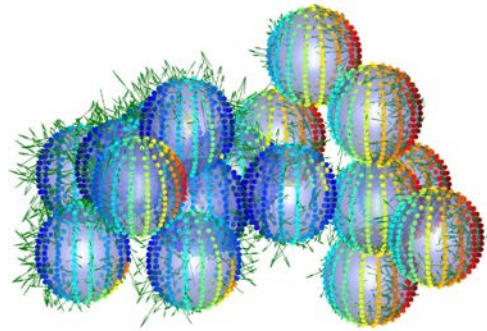


Figure 3. Gas molecules rebounding from a high surface temperature will transfer a higher amount of momentum versus gas molecules rebounding from shadow points. Above displays the momentum vectors for an aggregate. Thesis

vector are summed together and the photophoretic force is found.

III. RESULTS

Simulations were ran using the *OML-LOS code* and the *Dynamics Code*. The simulations give the trajectory, the components and magnitude of the velocity, the components and magnitude of the acceleration, and the pressure on the surface for an isolated sphere.

A. Simulation One: Single Sphere, 5,000 counts

In the first simulation, the trajectory was plotted for a single sphere driven by Brownian motion. The goal of these simulations was to correctly model Brownian motion. In this certain simulation, we added a factor to the flux calculation and the trajectory is seen below.

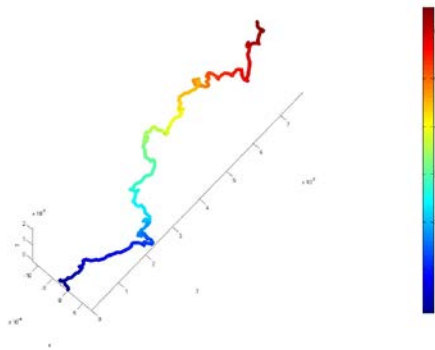


Figure 4. This is a trajectory of a single sphere which is assumed to be driven by the random force from Brownian motion. The color represents the time of the simulation, where blue is the start and red is the end of the simulation.

As we can see, the sphere seems to be somewhat random but tends to go in a defined direction. This definite direction is not completely analogous to Brownian motion.

B. Simulation Two: Single Sphere, 5,000 counts

The difference between this simulation and the last one is that the rebound direction was calculated in a different manner. The trajectory of the sphere was then mapped for 5,000 counts. In addition to the trajectory of the sphere being calculated, we plotted the components of the velocity versus the components of the acceleration.

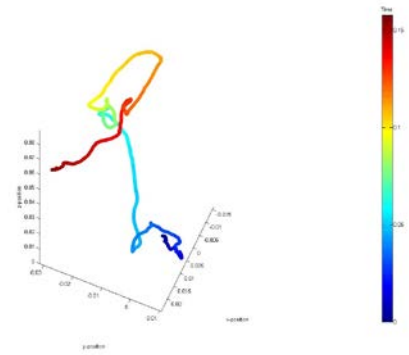


Figure 5. This is a trajectory of a single sphere, using a new rebound direction which is assumed to be driven by the random force from Brownian motion. The color represents the time of the simulation, where blue is the start and red is the end of the simulation.

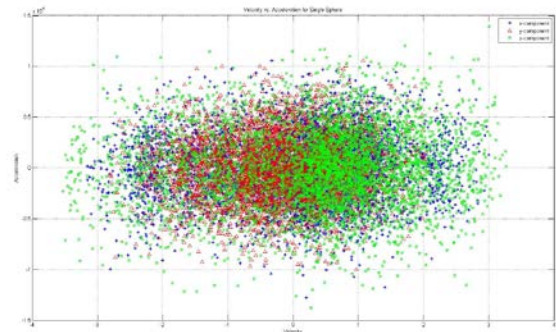


Figure 6. This is a plot of the components of velocity versus the components of the acceleration. The colors blue, red, and green represent the x-component, the y-component, and the z-component, respectively.

The trajectory of the single sphere seems more random than the previous simulation. There is still a definite direction in the motion of the sphere, in this case, the sphere tends to move in the z-direction. This makes more sense when looking at figure 6, in that the z-components tend to have a positive velocity no matter having a positive or negative acceleration.

C. Simulation Three: Single Sphere, 5,000 counts

The difference from this simulation and the past simulations is that the order in which the forces were calculated in the *Dynamics code* were reordered, giving a more correct way in determining the new position, velocity, and acceleration of the sphere at each time step. The trajectory of the sphere is seen in figure 7. The components of the velocity with respect to time was plotted to see how the velocity acts over time. The components of the acceleration was also plotted with respect to time.

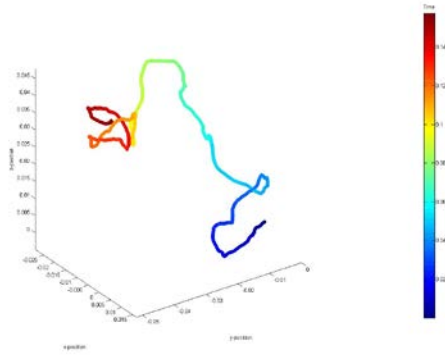


Figure 7. This is a trajectory of a single sphere which is assumed to be driven by the random force from Brownian motion. The color represents the time of the simulation, where blue is the start and red is the end of the simulation.

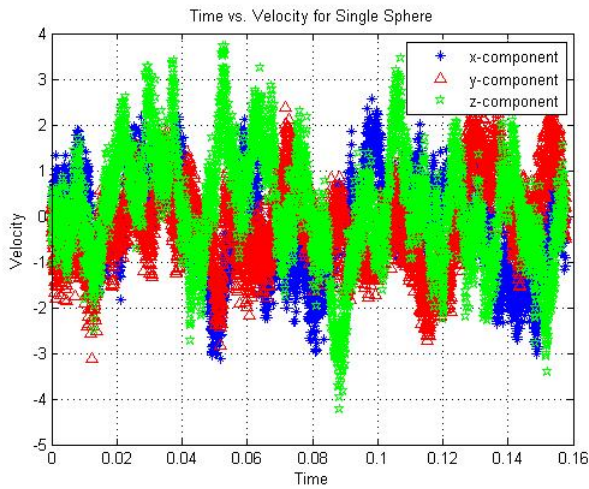


Figure 8. The components of the velocity is plotted with respect to time. The y-component and the z-component of the velocity tend to fluctuate, but the x-component tend to stay positive.

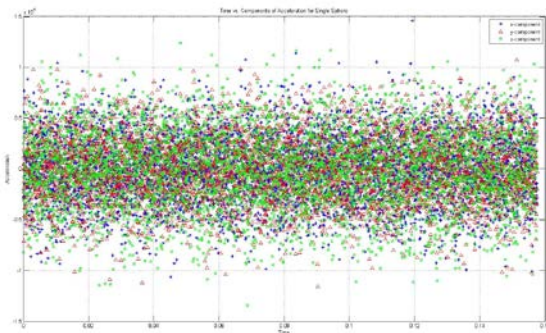


Figure 9. The components of the acceleration are plotted with respect to time. The randomness of the accelerations relate to the accelerations due to Brownian motion.

The pressure of the gas is measured to be about 400 Pa. The pressure on the surface of the sphere was then calculated and plotted with respect to time. We should see that the pressure on the surface of the sphere matches the pressure of the gas.

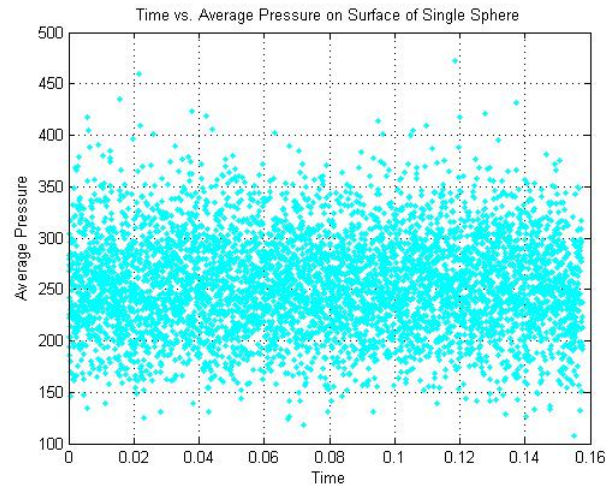


Figure 10. The pressure of the sphere is calculated at each time step and plotted. The range of the surface pressure range from 200-300 Pa.

IV. CONCLUSIONS

The initial simulations of tracking the trajectories of aggregates due to the photophoretic forces were incorrect due to the fact that the Brownian motion model was incorrect. Closer observations for modeling Brownian motion was taken. The model was changed from an aggregate to a single sphere and then tracked the forces on that isolated sphere. The trajectories of the single sphere due to Brownian motion did not appear random. Brownian motion is driven by a random force and thus has a random trajectory. The randomness in our model was slight and did not measure up to the experimental data from Blum et al 1996.

The pressure of the gas was measure to be around 400 Pa. The pressure on the surface of the sphere was calculated and was around 255 Pa on average. The pressure on the surface of the sphere is about one and a half less than it should be. More work needs to be done in order to resolve the pressure difference between the gas and the surface pressure.

In the final set up simulations, the trajectories of sphere were done at 70 counts. The final set included three simulations of the trajectory of an isolated sphere. The difference in each simulation is the total number of point on the surface of the sphere. The points on the sphere went from 36 to 64 to 256. The reason why the counts dropped from 5,000 to 70 is that the randomness from Brownian motion should be seen at lower counts. The trajectories of each sphere does not change despite the change in the number of points on the surface of the sphere.

Future work will include resolving the Brownian motion model, then the photophoretic force can be calculated correctly for both aggregates and isolated spheres.

V. ACKNOWLEDGMENTS

Special thanks to Dr. Lorin Matthews, Dr. Truell Hyde, Raziye Yousefi, and CASPER, Center for Astrophysics, Space physics, and Engineering Research. This material is based upon work supported by the National Science Foundation under Grant No. 1262031.

VI. REFERENCES

- Blum, Jürgen, and Gerhard Wurm. "The growth mechanisms of macroscopic bodies in protoplanetary disks." *Annu. Rev. Astron. Astrophys.* 46 (2008): 21-56.
- Levasseur-Regourd, A. C., M. Zolensky, and Jérémie Lasue. "Dust in cometary comae: Present understanding of the structure and composition of dust particles." *Planetary and Space Science* 56.13 (2008): 1719-1724.
- Ma, Qianyu, et al. "Charging of aggregate grains in astrophysical environments." *The Astrophysical Journal* 763.2 (2013): 77.
- Matthews, L. S., Victor Land, and T. W. Hyde. "Charging and coagulation of dust in protoplanetary plasma environments." *The Astrophysical Journal* 744.1 (2012): 8.
- Okuzumi, Satoshi. "Electric charging of dust aggregates and its effect on dust coagulation in protoplanetary disks." *The Astrophysical Journal* 698.2 (2009): 1122.
- Rohatschek, Hans. "Semi-empirical model of photophoretic forces for the entire range of pressures." *Journal of aerosol science* 26.5 (1995): 717-734.
- Tehrani, Shahram, et al. "Photophoresis of micrometer-sized particles in the free-molecular regime." *International journal of heat and mass transfer* 44.9 (2001): 1649-1657.
- Teiser, Jens, Ilka Engelhardt, and Gerhard Wurm. "Porosities of protoplanetary dust agglomerates from collision experiments." *The Astrophysical Journal* 742.1 (2011): 5.
- Testi, Leonardo, et al. "Dust Evolution in Protoplanetary Disks." *arXiv preprint arXiv:1402.1354* (2014).
- van Eymeren, Janine, and Gerhard Wurm. "The implications of particle rotation on the effect of photophoresis." *Monthly Notices of the Royal Astronomical Society* 420.1 (2012): 183-186.
- van Eymeren, Janine, and Gerhard Wurm. "The implications of particle rotation on the effect of photophoresis." *Monthly Notices of the Royal Astronomical Society* 420.1 (2012): 183-186.
- Wada, Koji, et al. "Collisional growth conditions for dust aggregates." *The Astrophysical Journal* 702.2 (2009): 1490.
- Weidenschilling, S. J. "The distribution of mass in the planetary system and solar nebula." *Astrophysics and Space Science* 51.1 (1977): 153-158.
- Weidenschilling, S. J. "The origin of comets in the solar nebula: A unified model." *Icarus* 127.2 (1997): 290-306.
- Wurm, Gerhard, Mario Trieloff, and Heike Rauer. "Photophoretic Separation of Metals and Silicates: The Formation of Mercury-like Planets and Metal Depletion in Chondrites." *The Astrophysical Journal* 769.1 (2013): 78.
- Wurm, Gerhard, Mario Trieloff, and Heike Rauer. "Photophoretic Separation of Metals and Silicates: The Formation of Mercury-like Planets and Metal Depletion in Chondrites." *The Astrophysical Journal* 769.1 (2013): 78.